Chemical reactions rectify mixtures composition

Emilie Guilbert[1] and Emmanuel Villermaux[1,2,*]

[1]*Aix Marseille Université, CNRS, Centrale Marseille, IRPHE UMR 7342, 13384 Marseille, France*
[2]*Institut Universitaire de France, 75005 Paris, France*

We show how the overall concentration distribution of the product in a randomly stirred reactive mixture is modified by the chemical reaction. We decipher the intermingled effects of stretching enhanced diffusion and chemical production on the evolution of each concentration level, and show why chemical kinetics contributes to a "rectification" mechanism when low concentration levels grow faster than higher ones. The rectification amounts to a compression of the product concentration distribution, which is found to be narrower around its mean than for a pure, nonreactive scalar. This phenomenon is illustrated through a series of quantitative experiments in which scalar mixing and the effects of the reaction are measured concomitantly, but independently.

Chemical reactions are obviously sensitive to the way the medium in which they occur is stirred [1,2]. In chemical reactors for instance, that the net outcome of a chemical reaction with nonlinear kinetics is influenced by the rotation speed of the impeller [3,4], and even by its sense of rotation [5], is a well-known fact [6], as well as the impact of stirring on the concentration spectra in turbulent mixtures [7]. Less obvious is the question of the influence of the chemical reaction itself on the final *composition* of the reacted mixture: For a given chemical reaction between, say, two initially segregated reactants, will a vigorous stirring produce a more, or less homogeneous product concentration distribution, than a gentle stirring protocol? And then, what does gentle/vigorous mean, and what do we mean by stirring? Examples abound showing that, in most instances involving a mixing operation, it is not the mean, nor even the standard, deviation of the mixture composition that is of interest, but rather the probability of an extreme concentration event (see Ref. [8] and references therein). This is the reason why understanding the overall reaction product concentration distribution is, besides being intellectually challenging and the subject of several modeling approaches in various contexts [9,10], paramount.

We investigate these questions on hand of a newly documented chemical reaction [11] between two transparent reactants, namely fluorescin (labeled A) and potassium ferricyanide (labeled B), producing fluorescein (labeled F) which is fluorescent in water. This second-order irreversible reaction A + 2 B → F with reaction constant k has a production rate per unit volume $\dot{c} = k\, c_A c_B$ (the c_i's denote the reactants concentrations, and $c \equiv c_F$ that of the product F) and when the initial concentrations are such that, say, $c_{B0}/c_{A0} \gg 1$, the reaction kinetics is of a pseudo-first-order type defining the reaction time τ as (see Ref. [11] for details)

$$\tau = (k\, c_{B0})^{-1}, \quad \text{giving} \quad \dot{c} = -\dot{c}_A = \frac{c_A}{\tau}. \tag{1}$$

*emmanuel.villermaux@univ-amu.fr

As for stirring, we use the protocol introduced by Villermaux and Duplat [12,13] consisting of stirring a blob of dye with a rod in a thin layer of a diluting very viscous fluid, in a two-dimensional, bounded, quasiperiodic fashion [see Supplemental Material (SM) [14]]. That protocol is typical of those where the mixture is directed toward uniformity by sequential random interactions between its subparts [8], for which the distribution $p(c, t)$ of the dye concentration c obeys, for a conserved scalar ($\tau \to \infty$)

$$\partial_t p = -\partial_c(\dot{c}\, p) + \dot{n}(-p + p^{\otimes 1+1/n}), \tag{2}$$

$$\dot{c} = -(\dot{n}/n)c \tag{3}$$

providing the amplitudes of the concentration fluctuations of c around its constant mean $\langle c \rangle$ as (see SM)

$$p(x = c/\langle c \rangle) = \frac{n^n}{\Gamma(n)} x^{n-1} e^{-nx}, \tag{4}$$

which indeed describes uniformity $p(x) \to \delta(x - 1)$ as $n \to \infty$. The parameter n is an increasing function of time. It varies exponentially [15], or as a power law [12,16,17], depending on the precise stirring protocol.

In a reactive mixture (τ finite), the product concentration is not only subjected to stretching enhanced diffusive damping [18], but also to chemical production so that Eq. (3) now incorporates the source term given in Eq. (1) as

$$\dot{c} = -\frac{\dot{n}}{n} c + \frac{1}{\tau}(c_{A0} - c) \tag{5}$$

when A is the limiting reactant. We explore in this Letter the consequence of this additional source on the shape of the product concentration distribution.

The reactants A and B are transparent and F is a fluorescent product. We also make use of a passive conserved scalar, namely rhodamine (labeled R) which is not involved in the reaction, but is a useful tracer to probe the mixing properties of the stirring protocol, concomitantly but independently of the ongoing reaction. All solutions are prepared from the same working fluid (a mixture of water and UCON oil [19]) having a viscosity 8×10^{-1} Pa s setting the species diffusion coefficients: $D_A = D_F = 1 \times 10^{-11}$ m^2 s^{-1}, $D_B = 4 \times 10^{-11}$ m^2 s^{-1}, and $D_R = 2.9 \times 10^{-11}$ m^2 s^{-1}. The solutions' temperature $T = 23\,°C$, $pH = 12$, and the initial concentrations $c_{R0} = 4 \times 10^{-6}$ mol ℓ^{-1} and $c_{A0} = 2 \times 10^{-5}$ mol ℓ^{-1} are kept constant. The chemical time τ is varied through c_{B0} according to Eq. (1).

The experiment consists in stirring a blob of A+R deposited in a thin layer of B, with a rod. A number of parallel cuts is made in one direction and then the same number in the orthogonal direction, with this operation defining one cycle (Fig. 1 and SM), and we proceed sequentially. As in Ref. [12], the state of the mixture is recorded cycle after cycle (Figs. 1 and 2). The whole stirred layer is uniformly illuminated from the top by an expanded argon-ion laser beam operating in multimode, namely emitting at 488 nm (thus exciting the green fluorescence of F) and at 514 nm (exciting the red fluorescence of R), allowing for the fluorescein and rhodamine fields to be extracted independently by a color camera sensor. After calibration, these recorded fields are converted into molar concentrations (see Ref. [20] and SM). The stirring rod diameter is $s_0 \approx 2$ mm, and its displacement speed along the liquid layer $u \approx 10$ cm s^{-1} so that the Péclet number in this protocol is Pe $= u\, s_0/D_F \approx 10^7$, much larger than unity.

Mixing proceeds in this system by the formation of lamellae which are linearly stretched at the passage of the rod, and which are forced to overlap because stirring takes place in a confined environment [16]. The time t_s it takes for the species to mix at the molecular level is in that case such that $u\, t_s/s_0 \sim$ Pe$^{1/3}$ [12,18,21], of the order of $t_s \simeq 3$ s. Local molecular mixing at the passage
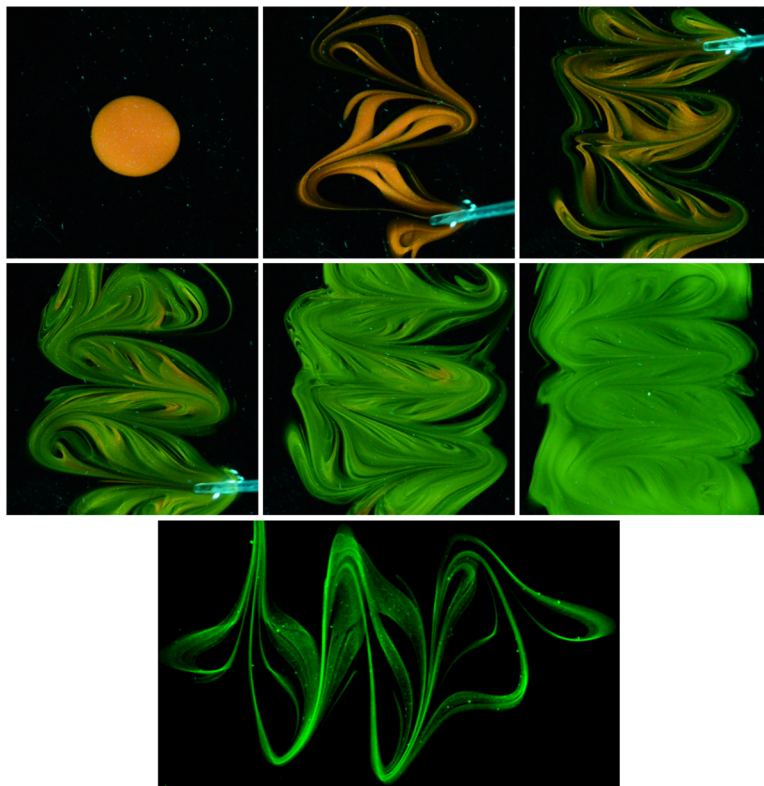
FIG. 1. Top: Mixing of a blob of A+R (fluorescin+rhodamine) in a solution of B (ferricyanide). Concentration fields of R (red) and F (green) after 0, 1, 3, 4, 5, and 8 stirring cycles. The reaction time is $\tau \simeq 8\,\text{s}$ for $c_{B0} = 1.5 \times 10^{-1}\,\text{mol}\,\ell^{-1}$. Bottom: Example of a fluorescein pattern produced by the mixing of a blob of A in a solution of B after 1 stirring cycle (same conditions as above) showing the organization of the field as overlapping lamellae.

of the rod is vigorous in the sense that the Damköhler number [22,23],

$$\text{Da} = \frac{t_s}{\tau}, \tag{6}$$

is usually smaller than unity so that chemical production is reaction limited in the molecularly mixed regions [11,24].

Figure 2 shows the course of a typical experiment: As the A+R blob is deposited in the B layer, only the fluorescence of R is visible and as the number of stirring cycles increases, the blob elongates in stretched lamellae which disperse and overlap in the diluting B layer. The fluorescence of the reaction product F progressively intensifies, first at the lamellae borders, where diffusive interpenetration occurs, before invading the whole dispersed area. The reaction product locations highlight the regions of molecular mixing between A (and therefore R as well), and B.

Successive distributions of the passive rhodamine $p(c_R/\langle c_R \rangle)$ are plotted in Fig. 2; they present the skewed bell shape, well fitted by the gamma distributions in Eq. (4) typical of the mixtures evolving by self-convolution, with conserved mean $\langle c_R \rangle$. The gamma order n_R increases with the number of cycles p (alternatively time t since $t = p \times t_{\text{cycle}}$ with $t_{\text{cycle}} = 5$ s) as $n_R \sim (t/t_s)^{3/2}$, as shown in Fig. 2 (see also Ref. [12]).

In the same experiment, the distributions of the product $p(c_F/\langle c_F \rangle)$ have a similar shape, also well adjusted by gamma distributions with, however, a measurably narrower width around the mean
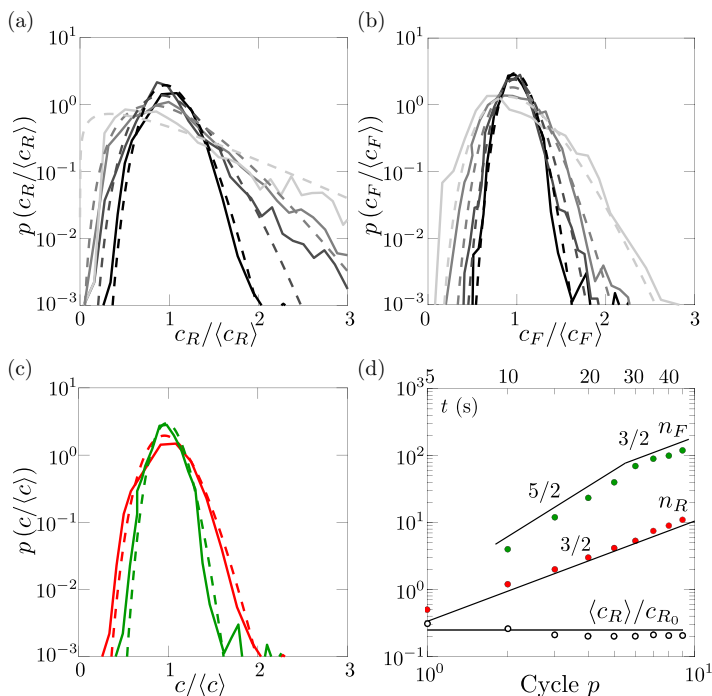
FIG. 2. Concentration distributions of (a) rhodamine $p(c_R/\langle c_R \rangle)$ and (b) of the product $p(c_F/\langle c_F \rangle)$ for the experiment in Fig. 1, at cycles 3, 4, 5, and 8 (solid lines). Fits by gamma distributions with orders n_R and n_F reported in (d). (c) Concentration distributions at cycle 8 for rhodamine (red) and the product (green) (dashed lines). (d) Fitting parameters n_R and n_F as a function of the number of cycles. Stirring is made at constant (conserved scalar) mean concentration $\langle c_R \rangle$.

$\langle c_F \rangle$ compared to the one of rhodamine at the same time. The average product concentration $\langle c_F \rangle$ also now obviously increases in time. The corresponding gamma orders n_F are larger than n_R because they increase faster in time (Fig. 2), typically as $n_F \sim t^{5/2}$. The presence of the reaction "speeds up" the approach to uniformity of the product mixture, which is "rectified" by comparison with a pure scalar under identical stirring. In addition, when the reaction is completed (at cycle 6 roughly), that is, when the A molecules have been all transformed in F, the reaction no longer has any effect on the F mixture composition, which then behaves as a passive scalar does, since we have $n_F \sim t^{3/2}$ from cycle 6 on, as seen in Fig. 2.

One way to understand the similarity (the distributions' shape) and the difference (their width) between the passive scalar, and the reactive cases is as follows: Writing the evolution equation for $p(c, t)$ (here c denotes indifferently c_R when $\tau \to \infty$, and c_F for finite τ) in the Laplace domain $\tilde{p}(s, t) = \int e^{-sc} p(c, t) dc$ with the full drift/production term in Eq. (5) gives

$$\partial_t \tilde{p} = -\left(\frac{\dot{n}}{n} + \frac{1}{\tau}\right) s\partial_s \tilde{p} - \frac{c_{A0}}{\tau} s\tilde{p} + \dot{n}(-\tilde{p} + \tilde{p}^{1+1/n}), \tag{7}$$

an equation which conserves the norm $\int p(c, t) dc = \tilde{p}(0, t) = 1$. Since diffusive damping and lamellae coalescence are features solely associated with scalar stirring, we have $n \equiv n_R$. The distribution *shape* is set by the self-convolution term in Eq. (2) only, which produces gamma distributions [12,16], a common feature thus expected for both the passive and reactive cases, consistent with our observations in Fig. 2. The average concentration $\langle c \rangle = -\partial_s \tilde{p}|_{s=0}$ and variance $\langle c^2 \rangle = \partial_s^2 \tilde{p}|_{s=0}$ are such that the mixture mean-squared standard deviation $\sigma^2 = \langle c^2 \rangle - \langle c \rangle^2$ evolves
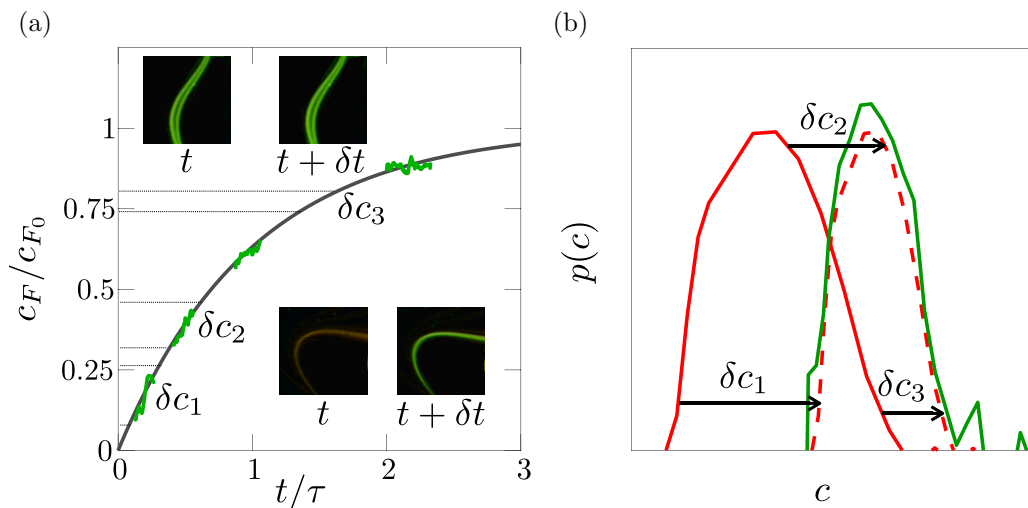
FIG. 3. (a) Master chemical kinetic curve in Eq. (11) on which is superimposed the evolution of the concentrations in F of four filaments between two cycle ($\delta t = 5$ s, $\tau = 8$ s) showing their distinct evolutions depending on their initial concentration. (b) The "rectification" mechanism: Starting from a given measured R concentration distribution (red curve), the F distribution is inferred by computing the increments δc from Eq. (12), which add up to each concentration level c_R to obtain the c_F's an instant of time δt later (dashed red) and, by normalization, the (measured) F distribution (green curve). The anamorphosis of the initial red curve consists in a translation, plus a compression due to the convexity of the master curve.

as (see SM)

$$\frac{\partial_t \sigma^2}{\langle c \rangle^2} = -\frac{\dot{n}}{n}\left(\left[1 + \frac{2n}{\tau \dot{n}}\right]\frac{\sigma^2}{\langle c \rangle^2} - \frac{1}{n}\right). \tag{8}$$

A property of gamma distributions is that the standard deviation scaled by the mean squared is equal to the inverse of their order [25]. We thus have, for the product field $\sigma^2/\langle c \rangle^2 = n_F^{-1}$, and, asymptotically from Eq. (8),

$$n_F = n_R\left(1 + \frac{2n_R}{\tau \dot{n}_R}\right) \tag{9}$$

or

$$n_F = \left(\frac{t}{t_s}\right)^{3/2}\left(1 + \frac{3t}{\tau}\right), \tag{10}$$

which indeed features a faster increase $n_F \sim t^{5/2}/(\tau t_s^{3/2})$ than for the scalar case [$n_R \sim (t/t_s)^{3/2}$] as soon as $t > \tau/3$, and is consistent with the pure scalar time dependence when $\tau \to \infty$.

Another, more direct way to reach the same result makes it clear the role of the reaction in the rectification process: In the regions where A and B are interpenetrated at the molecular scale (well mixed), the product concentration is given by Eq. (1),

$$c_F \equiv c(t) = c_{A0}(1 - e^{-t/\tau}), \tag{11}$$

or

$$\delta c = (c_{A0} - c)\frac{\delta t}{\tau}. \tag{12}$$

During a time interval δt, the concentration increment δc is larger in regions of low concentration ($c/c_{A0} \ll 1$) than in regions where the reaction is close to finished ($c/c_{A0} \lesssim 1$); the concentration
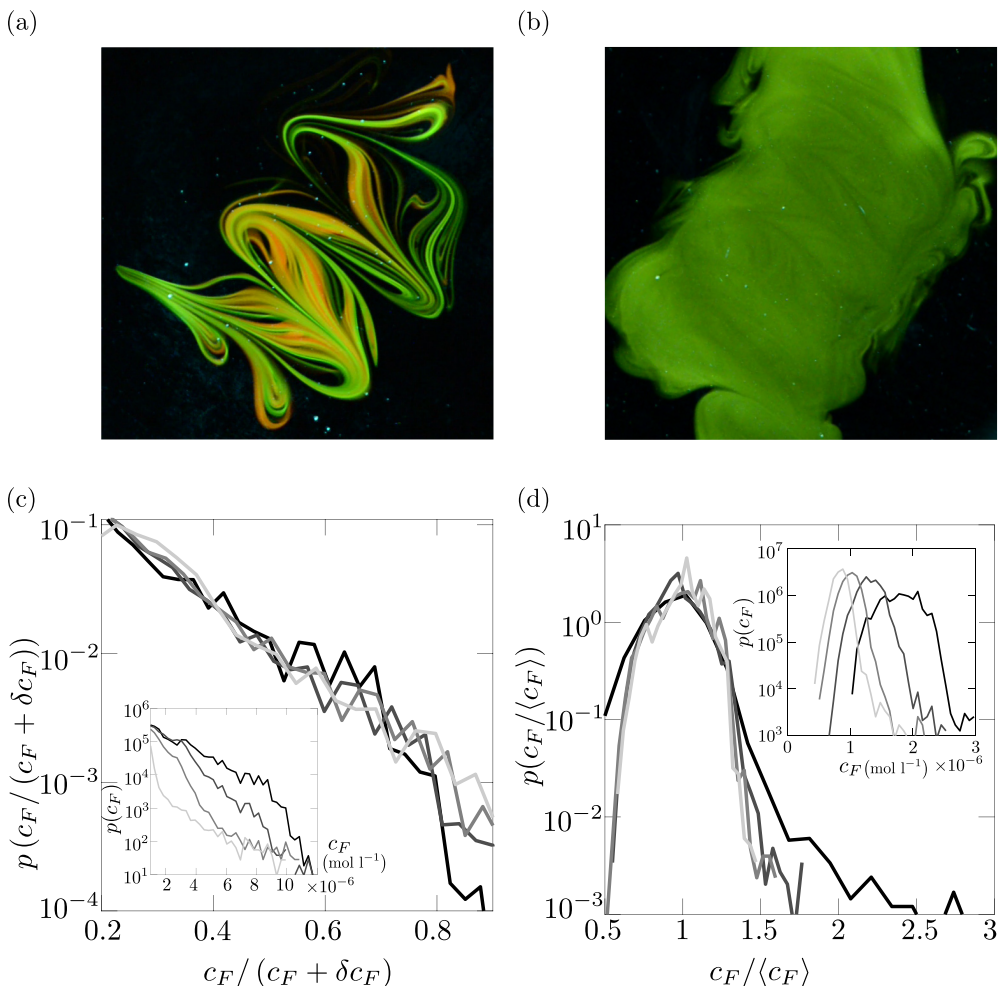
(a)

(b)

(c)

(d)

FIG. 4. Patterns of c_F obtained at $t = 40$ s after (a) 1 cycle ($c_{B0} = 1.5 \times 10^{-1}$ mol ℓ^{-1}, $\tau \simeq 8$ s) and (b) 6 cycles ($c_{B0} = 1.5 \times 10^{-2}$ mol ℓ^{-1}, $\tau \simeq 80$ s). After 1 cycle, the distributions $p(c_F)$ are plotted in (c) for different times ($t = 0, \delta t, 2\delta t, 4\delta t$ with $\delta t = 10$ s) as a function of $c_F/(c_F + \delta c_F)$, with δc_F given by Eq. (12) to rescale the anamorphosis caused by the reaction (inset). After 6 cycles, the concentration distributions at $t = 0, 180, 360,$ and 540 s are well rescaled by the mean concentration $\langle c_F \rangle$ in the close-to-uniform mixture of (b).

speed $\delta c/\delta t$ along the concentration axis is a decreasing function of c itself, a consequence of the reaction kinetics in Eq. (1). This is in essence the rectification mechanism, where low concentration levels "catch up" to the higher ones by the sole action of the chemical reaction (Fig. 3). One readily sees that since $n^{-1}|_{t+\delta t} \sim [\langle c^2 \rangle - \langle c \rangle^2]_{t+\delta t}$, so that, with $\langle \delta c \rangle = (c_{A0} - \langle c \rangle)\frac{\delta t}{\tau}$ and $\langle c\delta c \rangle = (c_{A0}\langle c \rangle - \langle c^2 \rangle)\frac{\delta t}{\tau}$, we have, in a mixture about a composition state given by n_R,

$$\frac{\dot{n}_F}{n_R} = \frac{2}{\tau},$$ (13)

which is equivalent to Eq. (10). This scenario can be precisely checked by singling out lamellae with different concentrations in the mixture, and measuring their concentration increment δc given their initial concentration c at a given instant of time during the stirring protocol. These concentrations

lie on the master curve given by Eq. (11), and the increments are indeed smaller for larger c, as seen in Fig. 3.

For a given chemical time τ, the state of the mixture depends on the duration of the stirring protocol, the analog of the residence time in a continuous stirred reactor [26]. This fact is clearly apparent from the production/drift term in Eq. (5), the balance between drift on the concentration axis due to stretching $(-\dot{n}/n)$ and production rate by the reaction (τ^{-1}) being achieved when

$$\frac{n/\dot{n}}{\tau} = O(1), \tag{14}$$

namely when the macroscopic equivalent of the Damköhler number in Eq. (6) is of order unity. In the present case since $n \sim t^{3/2}$, the macroscopic Damköhler number is simply t/τ [11] and we have found in Eq. (10) that chemical kinetics rectifies the product concentration content as soon as $t/\tau > 1/3$. Figure 4(a) shows a very heterogeneous mixture after one cycle with $\tau \simeq 8$ s. After stirring, the transformation in Eq. (12) is needed to map the successive composition fields onto an invariant one. On the contrary, the reactants stirred for 6 cycles ($t \simeq 40$ s) with a slow reaction ($\tau \simeq 80$ s) are close to uniformly mixed when stirring stops, and a simple rescaling by the average concentration $\langle c_F \rangle$ maps the whole product distributions onto a single curve with large $n_F = 60$, as seen in Fig. 4(b).

Let us finally underline that the rectification phenomenology leading to a compression of the distribution about its mean is not particular to first-order reactions, but to all reactions with *positive* partial orders, namely those of the kind $\dot{c}_A \sim -c_A^\alpha$ with $\alpha > 0$. The curvature $\partial_t^2 c(t)$ of the master curve $c(t)$ has the sign of $-\alpha$ so that when $\alpha < 0$, larger increments δc are produced for larger c within δt, at the opposite of the situation investigated here. Although rare in nature, reactions with negative orders do occur [24] when multiple intermediate steps with radicals are involved, such as in the conversion of ozone O_3 into oxygen O_2 for instance ($2O_3 \rightarrow 3O_2$, see Ref. [27]). In an excess of O_2, the reaction kinetics analog to Eq. (1) is $kc_{O_3}^2/c_{O_2}$ with a partial order equal to -1 with respect to O_2. For these reactions, one expects, in line with the mechanism described in this Letter, that the distribution should broaden rater than compress around the mean, fostering the diversity of the concentration levels.

[1] P. V. Danckwerts, The effect of incomplete mixing on homogeneous reactions, Chem. Eng. Sci. **8**, 93 (1958).

[2] C. Dopazo and E. E. O'Brien, Isochoric turbulent mixing of two rapidly reacting chemical species with chemical heat release, Phys. Fluids **16**, 2075 (1973).

[3] S. Nagata, *Mixing, Principles and Applications* (Wiley, New York, 1975).

[4] J. C. Roux, P. De Kepper, and J. Boissonade, Experimental evidence of nucleation induced transition in a bistable chemical system, Phys. Lett. A **97**, 168 (1983).

[5] M. J. B. Hauser, D. Lebender, and F. W. Sneider, Stirring sense discriminates between stationary and oscillatory states, J. Chem. Phys. **97**, 2163 (1992).

[6] I. R. Epstein, Shaken, stirred—but not mixed, Nature (London) **346**, 16 (1990).

[7] S. Corrsin, The reactant concentration spectrum in turbulent mixing with a first-order reaction, J. Fluid Mech. **11**, 407 (1961).

[8] E. Villermaux, Mixing versus stirring, Annu. Rev. Fluid Mech. **51**, 245 (2019).

[9] R. O. Fox, *Computational Models for Turbulent Reacting Flows* (Cambridge University Press, Cambridge, UK, 2003).

[10] M. Dentz, T. Le Borgne, A. Englert, and B. Bijeljic, Mixing, spreading and reaction in heterogeneous media: A brief review, J. Contam. Hydrol. **120-121**, 1 (2011).

[11] E. Guilbert, C. Almarcha, and E. Villermaux, Chemical reaction for mixing studies, Phys. Rev. Fluids **6**, 114501 (2021).

[12] E. Villermaux and J. Duplat, Mixing as an Aggregation Process, Phys. Rev. Lett. **91**, 184501 (2003).

[13] J. Duplat, A. Jouary, and E. Villermaux, Entanglement Rules for Random Mixtures, Phys. Rev. Lett. **105**, 034504 (2010).

[14] See Supplemental Material at http://link.aps.org/supplemental/10.1103/PhysRevFluids.6.L112501 for experimental procedures, calibrations, and details of some calculations.

[15] P. Meunier and E. Villermaux, The diffusive strip method for scalar mixing in two-dimensions, J. Fluid Mech. **662**, 134 (2010).

[16] J. Duplat and E. Villermaux, Mixing by random stirring in confined mixtures, J. Fluid Mech. **617**, 51 (2008).

[17] T. Le Borgne, M. Dentz, and E. Villermaux, Stretching, Coalescence and Mixing in Porous Media, Phys. Rev. Lett. **110**, 204501 (2013).

[18] M. Souzy, I. Zaier, H. Lhuissier, T. Le Borgne, and B. Metzger, Mixing lamellae in a shear flow, J. Fluid Mech. **838**, R3 (2018).

[19] *UCON 75-H-90,000*, Available from DOW Company, Michigan, USA (2015).

[20] E. J. Marey, *Le Mouvement*, edited by G. Masson (Heinemann, London, 1895).

[21] P. Meunier and E. Villermaux, How vortices mix, J. Fluid Mech. **476**, 213 (2003).

[22] G. Damköhler, Der einfluss der turbulenz auf die flammengeschwindigkeit in gasgemischen, Z. Elektrochem. Angew. Phys. Chem. **46**, 601 (1940).

[23] D. A. Frank-Kamenetskii, *Diffusion and Heat Transfer in Chemical Kinetics* (Plenum Press, New York, 1969).

[24] M. Boudart, *Kinetics of Chemical Processes* (Prentice-Hall, Englewood Cliffs, NJ, 1968).

[25] W. Feller, *An Introduction to Probability Theory and Its Applications* (Wiley, New York, 1970).

[26] P. V. Danckwerts, Continuous flow systems, Chem. Eng. Sci. **2**, 1 (1953).

[27] S. Chapman, On ozone and atomic oxygen in the upper atmosphere, Philos. Mag. **10**, 369 (1930).